

Nanoengineered Electrically Contacted Enzymes on DNA Scaffolds: Functional Assemblies for the Selective Analysis of Hg²⁺ Ions

Gilad Mor-Piperberg, Ran Tel-Vered, Johann Elbaz, and Itamar Willner*

Institute of Chemistry, The Hebrew University of Jerusalem, Jerusalem 91904, Israel

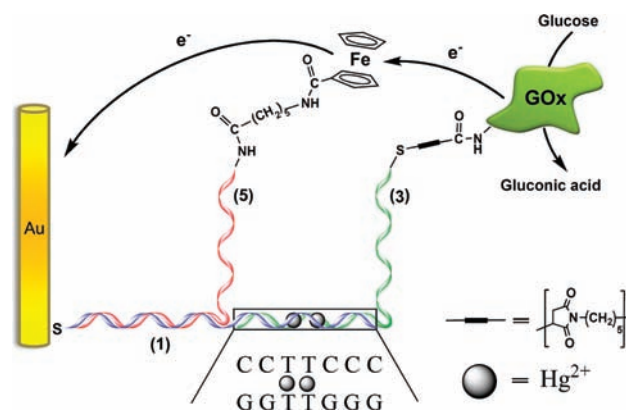
Received February 1, 2010; E-mail: willnea@vms.huji.ac.il

The electrical contacting of redox enzymes with electrodes is one of the most fundamental processes required for the development of bioelectronic devices, such as amperometric biosensors¹ or biofuel cells.² Recently, DNA monolayers assembled on electrodes were shown to act as templates for the organization of relay (cofactor) and enzyme units,³ leading to the controlled electrical contacting of the enzymes with the electrode. It is known that different ions form complexes with purine, pyrimidine, or artificial ligandoids in nucleic acid structures.⁴ For example, the formation of thymine–Hg²⁺–thymine (T–Hg²⁺–T) complexes is well-established.⁵ This feature has been used to develop different sensors for Hg²⁺ ions, which are a serious environmental pollutant.⁶ For example, the aggregation of oligothymine-functionalized Au NPs in the presence of Hg²⁺ led to a color transition due to interparticle plasmon coupling.⁷ Similarly, the luminescence of oligothymine-functionalized CdSe quantum dots was quenched by the formation of T–Hg²⁺–T complexes.⁸ Also, DNA molecular machines were activated by T–Hg²⁺–T complexes, leading to amplified optical detection of Hg²⁺ ions.⁹ In the present study, we demonstrate the use of a DNA scaffold for the amplified detection of Hg²⁺ using an electrically contacted relay/enzyme structure as a transducing element.

Scheme 1 outlines the configuration of the system. The thiolated nucleic acid (1) was assembled on a Au electrode [the surface coverage was estimated to be $(6.2 \pm 0.5) \times 10^{-11}$ mol cm⁻² using a quartz crystal microbalance (QCM) or Tarlov's electrochemical method¹⁰]. The enzyme glucose oxidase (GOx) was modified with the thiolated nucleic acid (2) to yield the GOx-modified nucleic acid (3). By absorbance spectroscopy, we estimated that ~ 2 units of (2) were linked per protein. The nucleic acids (1) and (3) include two mismatched T bases and five complementary G–C base pairs. While the five complementary G–C base pairs are insufficient to stabilize a duplex structure, a T–Hg²⁺–T complex is formed in the presence of Hg²⁺, and this acts cooperatively to stabilize the duplex between (1) and (3). The amine-functionalized nucleic acid (4) was reacted with ferrocene amidopentyl carboxylic acid succinimidyl ester to yield the ferrocene (Fc) relay-modified nucleic acid (5) that is complementary to the single-stranded domain of the scaffold (1). The number of base pairs between (5) and (1) is 12, and thus, a stable duplex between (5) and (1) exists. In the resulting tricomponent nucleic acid structure, the ferrocene unit acts as a relay that electrically contacts GOx with the electrode and activates the bioelectrocatalyzed oxidation of glucose. As the concentration of Hg²⁺ ions controls the extent of the biocatalyst associated with the electrode, the resulting bioelectrocatalytic currents were anticipated to correlate with the concentration of Hg²⁺. Also, since the formation of the T–Hg²⁺–T complex is coupled to a biocatalytic system, the recognition of Hg²⁺ ions is amplified by the bioelectrocatalytic process.

The hybridized Fc-functionalized nucleic acid (5) shows a quasi-reversible redox wave at 0.05 V [vs Ag quasi-reference electrode

Scheme 1. Bioelectrocatalytic Activation of Glucose Oxidation by a Hg²⁺-Bridged DNA Nanostructure Consisting of a Ferrocene Relay and Glucose Oxidase on a Nucleic Acid Template Associated with an Electrode (the Nucleic Acid Sequences Are Detailed in the SI)



(QRE)] that is characteristic of a surface-confined redox species with a Fc surface coverage of $(2.1 \pm 0.1) \times 10^{-11}$ mol cm⁻² determined by QCM and $(2.6 \pm 0.3) \times 10^{-11}$ mol cm⁻² by coulometric analysis of the Fc redox wave [see Figure S1 in the Supporting Information (SI)]. Figure 1A shows the cyclic voltammograms of the (1)/(3)/(5)-modified electrode upon interaction with Hg²⁺ ions (1 μ M) for 30 min in the presence of various concentrations of glucose. Bioelectrocatalytic currents were observed, and these intensified as the concentration of glucose was increased. The calibration curve corresponding to the amperometric responses of the modified electrode at different glucose concentrations is shown in the Figure 1A inset. Several control experiments were performed to characterize the system and elucidate the functions of the different components in the bioelectrocatalytic process. Substitution of the nucleic acid-modified GOx, (3), with a foreign nucleic acid-functionalized GOx, (3a), that does not hybridize with the template (1) did not lead to any bioelectrocatalytic oxidation of glucose. This implies that the assembly of GOx on the template is essential to stimulate the electrochemical oxidation of glucose, and that it is formed only by the T–Hg²⁺–T bond. In a further experiment, the nucleic acid-tethered Fc, (5), was excluded from the system. Under these conditions, the bioelectrocatalytic process was blocked (see Figure S2). This result implies that the Fc unit acts as a relay that mediates the electron transfer between the enzyme's redox site and the electrode. Furthermore, while previous reports have indicated that the adenine base binds to Au surfaces,¹¹ we found by QCM and cyclic voltammetry experiments that the oligoadenine sequences associated with (5) and (3) do not bind to the electrode in the absence of the scaffold (1). The kinetics of the (1)/(3)/(5)-modified electrode was investigated (Figure 1B). The bioelectrocatalytic responses of the system intensified as the time of interaction with Hg²⁺ ions increased, and they leveled off to a saturation value after ~ 30 min.

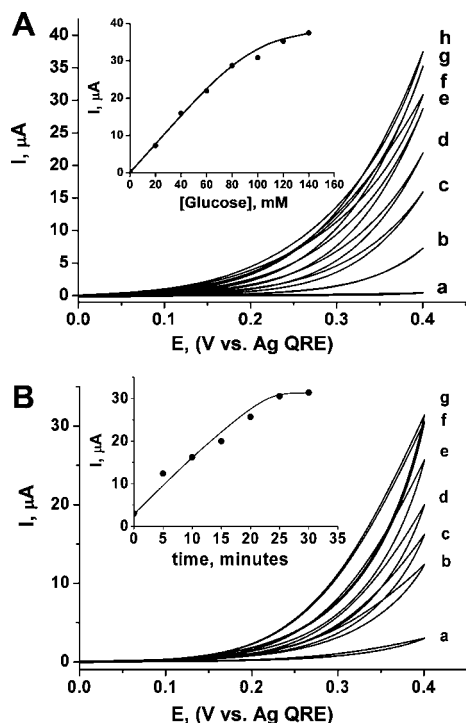


Figure 1. (A) Cyclic voltammograms corresponding to the bioelectrocatalytic oxidation of glucose by the nucleic acid-tethered ferrocene, (5), and the nucleic acid-tethered GOx, (3), assembled on the DNA template (1) linked to a Au electrode in the presence of 1 μM Hg^{2+} at an incubation time of 30 min with various concentrations of glucose: (a) 0, (b) 20, (c) 40, (d) 60, (e) 80, (f) 100, (g) 120, (h) 140 mM. Inset: Derived calibration curve at $E = 0.4$ V vs Ag QRE. (B) Time-dependent amperometric responses of the DNA/Fc/GOx construct in the presence of 1 mM Hg^{2+} and 100 μM glucose after (a) 0, (b) 5, (c) 10, (d) 15, (e) 20, (f) 25, (g) 30 min. All of the measurements were recorded at a scan rate of 10 mV s^{-1} in a HEPES buffer (10 mM, pH 7.4) that included 50 mM NaNO_3 .

Accordingly, all subsequent analyses of Hg^{2+} ions used a time interval of 30 min of incubation. The system was then used to analyze Hg^{2+} ions. Figure 2A shows the cyclic voltammograms generated by the tricomponent assembly of nucleic acids in the presence of 100 mM glucose and various concentrations of Hg^{2+} . As the concentration of Hg^{2+} ions was elevated, the electrocatalytic currents intensified. The resulting calibration curve is depicted in the inset of Figure 2A. The detection limit for analyzing Hg^{2+} corresponded to 100 ± 10 pM (see the SI). The resulting detection limit is improved by a factor of 10^2 – 10^3 relative to Hg^{2+} sensors implementing metal or semiconductor nanoparticles.^{8,9} This enhanced sensitivity originates from the amplification path provided by the biocatalytic system. A major aspect related to the sensing of Hg^{2+} by the enzyme–DNA structure concerns the specificity of the system. Figure 2B shows the current responses of the (1)/(3)/(5)-modified electrode in the presence of 100 mM glucose and various ions (1 μM). Evidently, the system reveals an impressive specificity toward the detection of Hg^{2+} ions. We further examined how the number of T– Hg^{2+} –T bridges, leading to the formation of the Hg^{2+} -bridged Fc/GOx nanostructure on the DNA scaffold (1), affects the bioelectrocatalytic functions of the system. We found that the use of a single T– Hg^{2+} –T bridge decreased the bioelectrocatalytic current by $\sim 60\%$ (see Figure S3). This result is consistent with the fact that the stability of the single T– Hg^{2+} –T-bridged nanostructure is lower, leading to a lower content of GOx on the electrode surface.

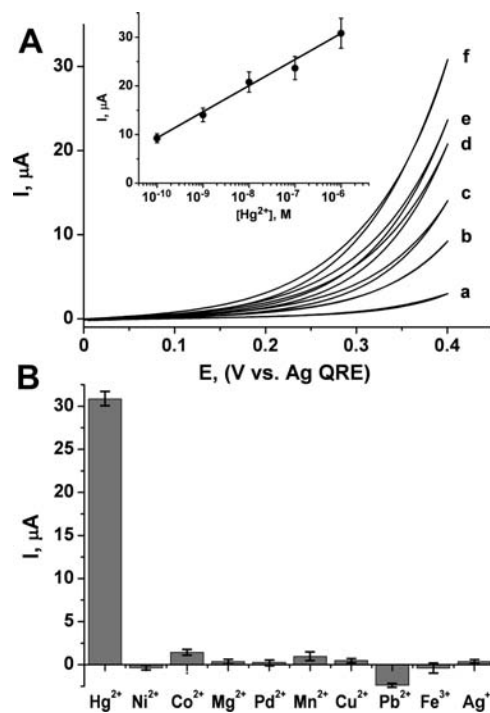


Figure 2. (A) Cyclic voltammograms corresponding to the bioelectrocatalytic oxidation of glucose using the Hg^{2+} -bridged Fc/GOx nucleic acid assembly in the presence of different concentrations of Hg^{2+} : (a) 0, (b) 0.1, (c) 1, (d) 10, (e) 100, (f) 1000 nM. Inset: semilogarithmic plot of the corresponding calibration curve ($E = 0.4$ V vs Ag QRE). The error bars correspond to a set of $N = 5$ experiments. (B) Selectivity in the analysis of Hg^{2+} ions by the bridged nanostructure. The concentration of each metal ion was 1 μM . Experimental conditions as in Figure 1. The incubation time for all ions was 30 min.

In conclusion, the present study has introduced a hybrid nucleic acid/protein structure for the sensing of Hg^{2+} . As other natural or synthetic bases⁴ selectively bind other metal ions (e.g., Ag^+ by cytosine), alternative sensing devices may be envisaged.

Acknowledgment. This research was supported by the Israel Science Foundation.

Supporting Information Available: Figures S1–S3 and experimental procedures. This material is available free of charge via the Internet at <http://pubs.acs.org>.

References

- (1) (a) Heller, A. *Curr. Opin. Biotechnol.* **1996**, *7*, 50. (b) Zayats, M.; Willner, B.; Willner, I. *Electroanalysis* **2008**, *20*, 583.
- (2) (a) Barton, S. C.; Gallaway, J.; Atanassov, P. *Chem. Rev.* **2004**, *104*, 4867. (b) Heller, A. *Phys. Chem. Chem. Phys.* **2004**, *6*, 209. (c) Willner, I.; Yan, Y.-M.; Willner, B.; Tel-Vered, R. *Fuel Cells* **2009**, *9*, 7.
- (3) (a) Piperberg, G.; Wilner, O. I.; Yehezkeili, O.; Tel-Vered, R.; Willner, I. *J. Am. Chem. Soc.* **2009**, *131*, 8724. (b) Fruk, L.; Müller, J.; Weber, G.; Narváez, A.; Domínguez, E.; Niemeyer, C. M. *Chem.–Eur. J.* **2007**, *13*, 5223.
- (4) Clever, G. H.; Kaul, C.; Carell, T. *Angew. Chem., Int. Ed.* **2007**, *46*, 6226.
- (5) Thomas, C. A. *J. Am. Chem. Soc.* **1954**, *76*, 6032.
- (6) Kiyake, Y.; Togashi, H.; Tashiro, M.; Yamaguchi, H.; Oda, S.; Kudo, M.; Tanaka, Y.; Kondo, Y.; Sawa, R.; Fujimoto, T.; Machinami, T.; Ono, A. *J. Am. Chem. Soc.* **2006**, *128*, 2172.
- (7) Lee, J. S.; Han, M. S.; Mirkin, C. A. *Angew. Chem., Int. Ed.* **2007**, *46*, 4093.
- (8) Freeman, R.; Finder, T.; Willner, I. *Angew. Chem., Int. Ed.* **2009**, *48*, 7818.
- (9) Li, D.; Wieckowska, A.; Willner, I. *Angew. Chem., Int. Ed.* **2008**, *47*, 3927.
- (10) Steel, A. B.; Herne, T. M.; Tarlov, M. *J. Anal. Chem.* **1998**, *70*, 4670.
- (11) Wolf, K. L.; Gao, Y.; Georgiadis, M. R. *Langmuir* **2004**, *20*, 3357.

JA1006355